

1 **$\delta^{18}\text{O}$ as a tracer of PO_4^{3-} losses from agricultural landscapes**

2

3 Naomi S. Wells^{1,2*}, Daren C. Gooddy³, Mustefa Yasin Reshid¹, Peter J. Williams³, Andrew C.
4 Smith⁴, Bradley D. Eyre¹

5

6 ¹Centre for Coastal Biogeochemistry, School of Environment, Science & Engineering, Southern
7 Cross University, PO Box 157, East Lismore, 2480 NSW, Australia

8 ²Department of Soil & Physical Sciences, Faculty of Agricultural & Life Sciences, Lincoln
9 University, Lincoln 7647, New Zealand

10 ³British Geological Survey, Wallingford, Oxfordshire, OX10 8BB, UK

11 ⁴British Geological Survey, Keyworth, Nottinghamshire, NG12 5GG, UK

12

13

14 *Author for correspondence: naomi.wells@lincoln.ac.nz

15

16 Submitted to *Journal of Environmental Management*

17

18 **Highlights**

- 19 • Isotope fingerprints of soil and fertiliser PO_4^{3-} ($\delta^{18}\text{O}_\text{P}$) vary within catchments
20 • Source mixing and biological turnover affect $\delta^{18}\text{O}_\text{P}$ signatures exported downstream
21 • Tracing agricultural pollution with $\delta^{18}\text{O}_\text{P}$ requires accounting for soil zone dynamics

22

23

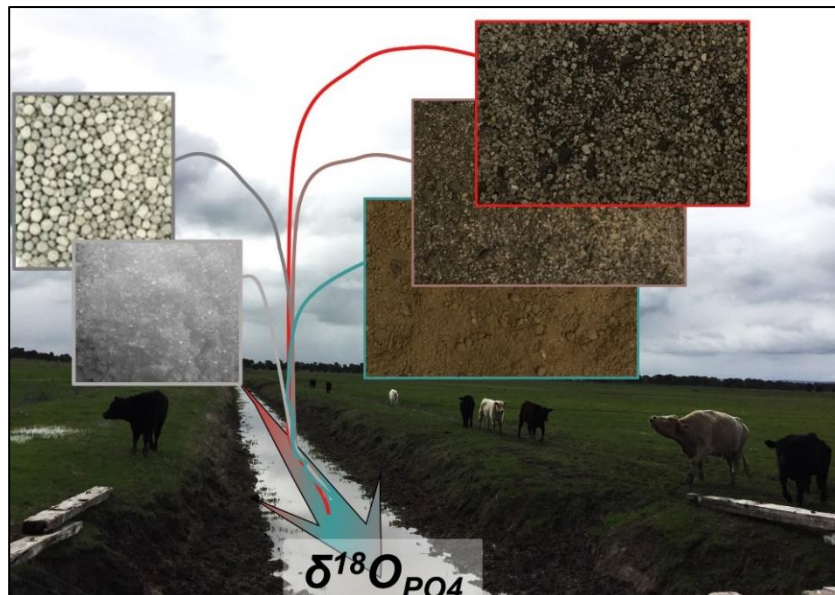
24

25

26

27 **Abstract**

28 Accurately tracing the sources and fate of excess PO_4^{3-} in waterways is necessary for sustainable
29 catchment management. The natural abundance isotopic composition of O in PO_4^{3-} ($\delta^{18}\text{O}_{\text{P}}$) is a
30 promising tracer of point source pollution, but its ability to track diffuse agricultural pollution is
31 unclear. We tested the hypothesis that $\delta^{18}\text{O}_{\text{P}}$ could distinguish between agricultural PO_4^{3-} sources by
32 measuring the integrated $\delta^{18}\text{O}_{\text{P}}$ composition and P speciation of contrasting inorganic fertilisers
33 (compound v rock) and soil textures (sand, loam, clay). $\delta^{18}\text{O}_{\text{P}}$ composition differed between the
34 three soil textures sampled across six working livestock farms: sandy soils had lower overall $\delta^{18}\text{O}_{\text{P}}$
35 values ($21 \pm 1 \text{ ‰}$) than the loams ($23 \pm 1 \text{ ‰}$), which corresponded with a smaller, but more readily
36 leachable, PO_4^{3-} pool. Fertilisers had greater $\delta^{18}\text{O}_{\text{P}}$ variability (~8‰) driven by both fertiliser type
37 and manufacturing year. Upscaling these values showed that ‘agricultural soil leaching’ $\delta^{18}\text{O}_{\text{P}}$
38 signatures could span from 18 – 25 ‰, and are influenced by both fertiliser type and the time
39 between application and
40 leaching. These findings
41 emphasise the potential of
42 $\delta^{18}\text{O}_{\text{P}}$ to untangle soil-
43 fertiliser P dynamics under
44 controlled conditions, but that
45 its use to trace catchment-
46 scale agricultural PO_4^{3-} losses
47 is limited by uncertainties in
48 soil biological P cycling and its associated isotopic fractionation.



49

50

51 **Keywords:** Phosphate leaching, stable isotope tracers, eutrophication, diffuse agricultural pollution,
52 Peel-Harvey catchment, $\delta^{18}\text{O}-\text{PO}_4^{3-}$

53

54

55 **1. Introduction**

56 Population growth and agricultural intensification has doubled phosphorus (P) inputs to
57 global rivers (Beusen et al., 2016). While point source (e.g., wastewater treatment plants) P
58 pollution can be effectively managed, diffuse P export from agriculture remains a pernicious water
59 quality threat (Haygarth et al., 2005). This is in part due to the difficulty tracing P from its origin
60 (e.g., fertiliser application) through the soil zone (where multiple biological and abiotic reactions
61 can occur) to the receiving waters (Melland et al., 2018). New tools to identify excess P transported
62 from soils to waterways via leaching and overland flow (henceforth ‘export’) are required to
63 mitigate aquatic ecosystem degradation from eutrophication (e.g., hypoxia, fish kills).

64 Calls to use the isotopic composition of oxygen within PO_4^{3-} ($\delta^{18}\text{O}_\text{P}$) as a P tracer date
65 back >10 years (Davies et al., 2014; Gruau et al., 2005; Young et al., 2009). This stems from
66 evidence that PO_4^{3-} sources (wastewater, tap water, fertilisers) can have distinct $\delta^{18}\text{O}_\text{P}$ signatures
67 (Goody et al., 2018; Goody et al., 2015; Granger et al., 2017b). Additionally, knowledge that
68 intracellular reactions with phosphatase enzymes impart a predictable temperature-dependent
69 equilibrium signature as oxygen is exchanged between PO_4^{3-} and the surrounding water (Chang and
70 Blake, 2015; Gross and Angert, 2015; Jaisi et al., 2011), means $\delta^{18}\text{O}_\text{P}$ can also indicate ecosystems
71 P cycling efficiency (Paytan et al., 2017; Pistocchi et al., 2017). Numerous studies propose using
72 $\delta^{18}\text{O}_\text{P}$ source and transformation data to constrain catchment-scale P pollution dynamics (Goody et
73 al., 2016; Granger et al., 2017b; Ishida et al., 2019; Tonderski et al., 2017). However, models are
74 limited by uncertainty around the $\delta^{18}\text{O}_\text{P}$ ‘signatures’ generated by different catchment P sources.

75 Controls on agricultural soil $\delta^{18}\text{O}_\text{P}$ values are poorly understood. This is a critical knowledge
76 gap as agricultural soils can dominate catchment P exports (Metson et al., 2017). Previous reviews
77 show soil $\delta^{18}\text{O}_\text{P}$ ranges from 11 – 25 ‰ (Tian et al., 2020), and that agricultural soil $\delta^{18}\text{O}_\text{P}$ tends
78 towards the higher end of the range predicted for biological equilibration with long-term soil water
79 trends (Granger et al., 2017a; Ishida et al., 2019; Polain et al., 2018; Tamburini et al., 2010; Tian et
80 al., 2020). Current models propose that systems reflect ‘source’ $\delta^{18}\text{O}_\text{P}$ values (e.g., fertilisers) when

81 PO₄³⁻ is in excess of biological demand, and shift towards equilibrium when PO₄³⁻ is limiting due to
82 enhanced P recycling (Bauke, 2020). Yet δ¹⁸O_P variability (~5‰ across a single paddock (Granger
83 et al., 2017a)) suggests additional factors are at play. And if P limitation were the main determinant
84 of δ¹⁸O_P reaching equilibrium, soil δ¹⁸O_P should correlate with PO₄³⁻ concentration, but this is not
85 typically observed (Granger et al., 2017a; Tamburini et al., 2010; Tian et al., 2020). Fertilisers
86 themselves cause further difficulty for defining the ‘agricultural’ δ¹⁸O_P range: fertiliser δ¹⁸O_P
87 composition is variable (Gruau et al., 2005), but could account for up to 80 % of agricultural soil
88 PO₄³⁻ exports (McLaren et al., 2016; Nash et al., 2019).

89 The aim of this study was to parameterise the potential of δ¹⁸O_P to trace agricultural PO₄³⁻
90 export at the catchment scale. We hypothesised that fertiliser inputs and soil P fertility combine to
91 create unique δ¹⁸O_P signatures. We tested this by measuring the δ¹⁸O_P composition of contrasting
92 fertilisers and soils across an 1,800 km² catchment, then using mixing models to define the possible
93 range of exported δ¹⁸O_P created by variable management (fertiliser application), biology (PO₄³⁻
94 turnover), and hydrology (time before leaching, equilibrium δ¹⁸O_P values).

95

96 **2. Materials & Methods**

97 2.1 Site description

98 Soil and fertiliser samples were collected from the 1,800 km² Peel-Harvey catchment in
99 southwestern Australia (Supporting Information (SI) S1 for maps). The catchment is flat (slope:
100 0.0015), with negligible elevation or aspect differences. Soils are P deficient, but their P retention
101 capacity varies with the underpinning geology: the alluvial soils have a clay texture and quickly
102 chemically immobilise fertiliser P inputs, while P is easily exported from the sand textured soils
103 formed on ancient dunes (Bolland and Allen, 1998; McArthur and Bettenay, 1974). The region has a
104 Mediterranean climate: hot, dry summers (27°C, 190 mm rain) v cool, wet winters (18°C, 1,000
105 mm rain). Fertilising to compensate for P immobilisation (clays) or leaching (sands) has contributed

106 to the hyper-eutrophication of the Peel-Harvey Estuary (Valesini et al., 2019). Pasture soils still
107 contain twice the optimal P range and leach 140 T P y⁻¹ (Rivers et al., 2013).

108

109 2.2 Sample collection

110 Fertiliser isotopic variability ($\delta^{18}\text{O}_{\text{P(fert)}}$) was constrained by analysing synthetic P fertilisers
111 from CSBP (Perth, Western Australia). These covered dominant fertiliser types: monoammonium
112 phosphate (MAP), superphosphate (SP), and a proprietary compound fertiliser with 16% N, 9% P,
113 14% S (AG). All three are water soluble (Nash et al., 2019). AG and SP were obtained for five
114 manufacturing years (2013-2017) and MAP from one year (2017). These fertilisers are the products
115 available to farmers in the catchment, but the exact mix applied to the sampled plots is unknown.

116 Soil samples (0 – 10 cm) were collected from 21 paddocks with contrasting soil textures
117 (clay, sand, loam) on six ~2 km² farms across the catchment (SI S1). Sampling was timed to winter
118 (July 2017) when soil PO₄³⁻ export occurs (Summers et al., 1999). Management effects, including
119 fertiliser contamination of the measured soil $\delta^{18}\text{O}_\text{P}$ composition ($\delta^{18}\text{O}_{\text{P(soil)}}$), were minimised by
120 selecting farms with the same land use (beef grazing) and vegetation (ryegrass/clover pasture)
121 participating in a multi-year P fertiliser minimisation trial. Triplicate samples (0-10 cm) spaced 10
122 m apart were collected over three transects from each paddock, and triplicates bulked to produce
123 three samples per paddock, which were homogenised, sieved, and air dried. Around this period ten
124 precipitation events were sampled for oxygen isotopes in water ($\delta^{18}\text{O}_{\text{H}_2\text{O}}$).

125

126 2.3 Sample analyses

127 All 63 soils (21 paddocks x 3 replicates) were analysed for pH, organic matter, and P
128 concentration. A subset of 25 soils, selected to cover the different farms and textures and using P
129 concentration to identify representative samples, were analysed for $\delta^{18}\text{O}_{\text{P(soil)}}$.

130 Soil pH was measured in 2.5:1 deionised water:dry soil extracts. Soil organic matter was
131 determined via ignition (550 C for 4 h), and total (P_{total}) and organic (P_{org}) P concentration measured

132 by extracting ignited v un-ignited soils with 1M H₂SO₄ (50:1) and measuring filtered extractant P
133 concentration via ICP (Saunders and Williams, 1955). Because chemical bonding between PO₄³⁻
134 and the soil matrix means that the amount of PO₄³⁻ in P_{total} may not correspond to the amount of
135 biologically available or leachable P, PO₄³⁻ concentrations were additionally measured in sequential
136 extractions as per (Hedley et al., 1982) in order to parameterise potential export and turnover rates.
137 This defines PO₄³⁻ by decreasing extractability as a proxy for availability (Gu and Margenot, 2020).
138 Briefly, 2 g dry soil were extracted with 40 ml deionised water, 0.5M NaHCO₃ (pH 8.5), 0.1M
139 NaOH, and 1M HCl. Tubes were agitated for 18 h (rotary shaker), centrifuged (15 minutes), filtered
140 (Whatman 0.45 µm) into duplicate 12 ml vials, stored at 4°C, and PO₄³⁻ concentrations analysed via
141 flow injection analysis after neutralising NaOH and NaHCO₃ extracts.

142 δ¹⁸O_{P(soil)} was measured on the total PO₄³⁻ extractable with 1M HCl (P_{TIP}). This enabled us
143 to directly compare values across strongly contrasting soil textures, as preliminary tests showed
144 clays had insufficient H₂O extractable PO₄³⁻ for δ¹⁸O_P analyses, while sands had insufficient PO₄³⁻
145 in the more tightly bound fractions. Using P_{TIP} is also advantageous because, by capturing the
146 majority of soil PO₄³⁻, it integrates the daily/seasonal P fluctuations observed in the more easily
147 extracted fractions (Angert et al., 2011). So while sequential chemical extractions are useful
148 indicators of the amount of soil PO₄³⁻ likely to be exported (Rupp et al., 2018) the P_{TIP} δ¹⁸O_{P(soil)}
149 provides a more robust and scalable soil ‘fingerprint’: extracted PO₄³⁻ ‘fractions’ not actually exist
150 in soils as discrete pools (Gu and Margenot, 2020) and do not reflect the potential biological
151 recycling over export-relevant timeframes (Helfenstein et al., 2020; Wang et al., 2021).

152 The δ¹⁸O_P compositions of soils ($n = 25$) and fertilisers ($n = 11$) were measured following
153 Tamburini et al. (2010) Extractions were carried out at BGS (Wallingford) and isotope analyses at
154 BGS (Keyworth). Briefly, 25 g dry soil (or 2 g fertiliser) were extracted overnight with 100 ml 1M
155 HCl, centrifuged, and filtered. Dissolved organic matter was removed with DAX resin (20 ml), then
156 ammonium phospho-molybdate precipitated with 4.2M ammonium nitrate and ammonium
157 molybdate (dissolved in ammonium citrate) and re-precipitated as magnesium ammonium

158 phosphate. After removing cations (AG50 X8 resin), silver phosphate (Ag_3PO_4) was precipitated
159 using 5 ml of silver ammine solution. Triplicate subsamples (300 μg) of the produced Ag_3PO_4 were
160 weighed into silver capsules and the $\delta^{18}\text{O}_P$ composition determined via thermal conversion
161 elemental analyser (TC-EA, ThermoFinnigan, Germany) at 1400°C with graphite and glassy carbon
162 chips, coupled to a Delta+XL mass spectrometer (ThermoFinnigan, Germany). Triplicates'
163 precision was $\leq 0.3\text{\%}$. Sample CO yield relative to Ag_3PO_4 standards was checked to ensure
164 deviations $< 10\text{\%}$. $\delta^{18}\text{O}_P$ values were calculated with an internal Ag_3PO_4 standard, ALFA-1 ($\delta^{18}\text{O}$:
165 14.2‰). There are no international reference materials, so ALFA-1 was calibrated to the Ag_3PO_4
166 standard 'B2207' (Elemental Microanalysis Ltd.) from an inter-laboratory comparison. Oxygen
167 isotope ($^{18/16}\text{O}$) values are reported in $\delta \text{\%}$ v VSMOW.

168

169 2.4 Calculations

170 Soil organic carbon (C_{org}) was estimated as $0.516 \times \text{loss-on-ignition}$ (Jensen et al., 2018).
171 Mineralisation of P_{org} to PO_4^{3-} , which can affect $\delta^{18}\text{O}_{\text{P(soil)}}$ values (Gross and Angert, 2015), was
172 parameterised as $\text{P}_{\text{min}(14)}$ (net mineralisation over 14 days) (Achat et al., 2010) based on measured
173 soil organic v inorganic P composition (see SI S2). Data analyses were performed using R.v4.0 /
174 RStudio.v1.3.959. Differences between farms and soil textures were determined via one-way
175 ANOVA with an estimated marginal means post-hoc (Bonferroni adjusted), and correlations
176 between soil parameters via Pearson's test (Kassambara, 2020). Figures were produced using
177 ggplot2, patchwork, and munsell (Pedersen, 2019; Wickham, 2018; Wickham, 2016). Significance
178 is defined as $p < 0.05$ and values are reported as mean \pm standard deviation.

179

180 2.4.1 Equilibrium $\delta^{18}\text{O}_P$

181 $\delta^{18}\text{O}_P$ values produced due to equilibrium fractionation during extracellular P cycling
182 ($\delta^{18}\text{O}_{\text{P(eq)}}$) were calculated using Eq. 1, as per (Chang and Blake, 2015; Hacker et al., 2019):

183 (Eq. 1)
$$\delta^{18}\text{O}_{\text{P(eq)}} = (\delta^{18}\text{O}_{\text{H}_2\text{O}} + 1000)e^{\left(\frac{14.43 * 1000}{T} - 26.54\right)/1000} - 1000$$

184 where $\delta^{18}\text{O}_{\text{P(eq)}}$ is defined by temperature (T, in kelvin) and $\delta^{18}\text{O}_{\text{H}_2\text{O}}$. Eq. 1 was solved two ways.
185 First, because the P_{TIP} used for $\delta^{18}\text{O}_{\text{P(soil)}}$ likely integrates long-term site conditions (Helfenstein et
186 al., 2018), $\delta^{18}\text{O}_{\text{P(eq)}}$ was calculated using long-term records of soil temperature at 10 cm (mean:
187 21°C, high: 26°C, low: 18°C) and $\delta^{18}\text{O}_{\text{H}_2\text{O}}$ (mean: -3.96 ‰, low: -2.74 ‰, high: -5.18 ‰, based on
188 monthly precipitation $\delta^{18}\text{O}_{\text{H}_2\text{O}}$ and amounts 1986-2012 for Perth, WA (Hollins et al., 2018;
189 IAEA/WMO, 2020)). Second, because loosely bound PO₄³⁻ in the sandy soils could be turning over
190 daily → seasonal intervals, $\delta^{18}\text{O}_{\text{P(eq)}}$ was also calculated using modelled daily winter soil
191 temperatures (mean: 13°C, high: 21°C, low: 8.2°C) (Kearney, 2019) and precipitation $\delta^{18}\text{O}_{\text{H}_2\text{O}}$
192 values measured during sampling ($\delta^{18}\text{O}_{\text{H}_2\text{O}}$: -3.07 ± 2 ‰, n = 10). Precipitation $\delta^{18}\text{O}_{\text{H}_2\text{O}}$ was
193 converted to soil water $\delta^{18}\text{O}_{\text{H}_2\text{O}}$ based on evidence that soil $\delta^{18}\text{O}_{\text{H}_2\text{O}}$ is a mass balance of seasonal
194 precipitation (Benettin et al., 2018), ± 3‰ evaporative enrichment (Sprenger et al., 2017; Wan and
195 Liu, 2016). See SI S3 for input data.

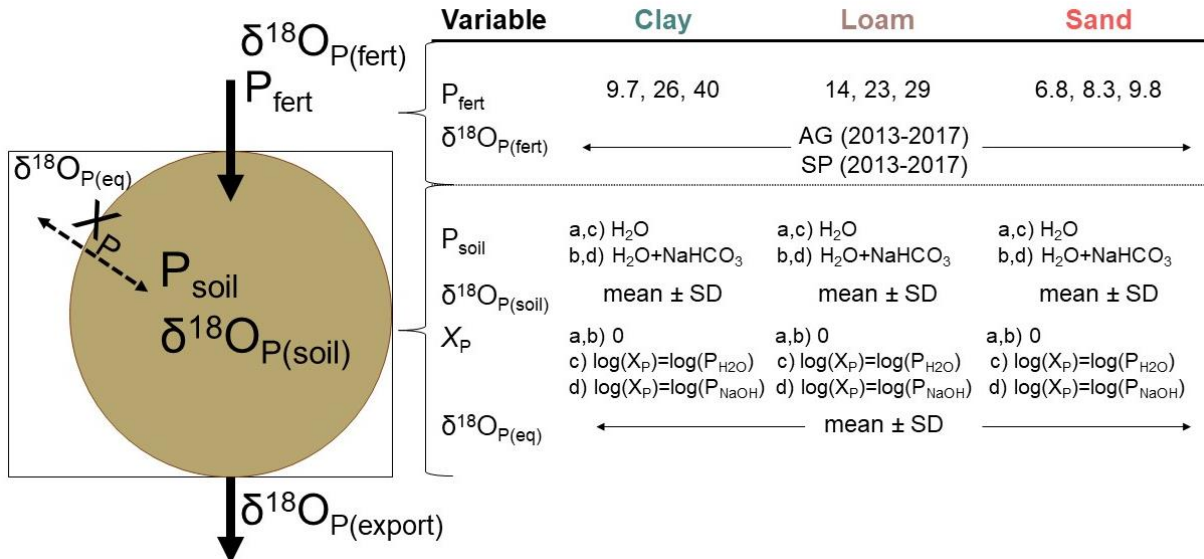
196

197 2.4.2 Export models

198 The possible $\delta^{18}\text{O}_{\text{P}}$ range exported from farms to waterways ($\delta^{18}\text{O}_{\text{P(export)}}$) was determined
199 using a two end-member mixing model that considered a range of fertilisers (type and application
200 rate), times between fertiliser application and PO₄³⁻ export, and soil biological P turnover (Fig. 1).

201

202



203

204 Fig. 1 Two-pool isotope mixing models (Eq. 2, Eq. 3) constrained the possible $\delta^{18}\text{O}_{\text{P}}$ range of PO_4^{3-} exported (leaching,
 205 run-off) from fertilised soils ($\delta^{18}\text{O}_{\text{P}(\text{export})}$). The model was solved using recommended low, moderate, and high fertiliser
 206 applications rate (P_{fert} , in $\mu\text{g P g}^{-1}$ soil) for each soil texture (clay, loam, sand) and $\delta^{18}\text{O}_{\text{P}(\text{fert})}$ values for two fertilisers
 207 (AG: N-P-K, SP: superphosphate) manufactured between 2013 and 2017. $\delta^{18}\text{O}_{\text{P}(\text{fert})}$ for each year \times fertiliser were
 208 ‘mixed’ with each soil texture using the measured $\delta^{18}\text{O}_{\text{P}(\text{soil})}$ range for P_{TIP} and P_{soil} ($\mu\text{g P g}^{-1}$ soil), defined by H_2O
 209 extractable PO_4^{3-} for fast export scenarios (a, c) and $\text{H}_2\text{O} + \text{NaHCO}_3$ extractable PO_4^{3-} for slow/seasonal export
 210 scenarios (b, d). $\delta^{18}\text{O}_{\text{P}(\text{export})}$ for both fast and slow export was calculated with (c, d) and without (a, b) soil biological P
 211 turnover (X_P), which shifts $\delta^{18}\text{O}_{\text{P}(\text{export})}$ towards $\delta^{18}\text{O}_{\text{P}(\text{eq})}$ (Eq. 1). Fast export X_P (c) was approximated by
 212 $[P_{\text{H}_2\text{O}} \cdot e^{(\log(100+P_{\text{H}_2\text{O}})/100 \cdot 1)}]/P_{\text{TIP}}$ and slow export X_P (d) by $[P_{\text{NaOH}} \cdot e^{(\log(100+P_{\text{NaOH}})/100 \cdot 1)}]/P_{\text{TIP}}$. Arrows indicate
 213 the same values were applied across all soil textures, otherwise soil-specific values (mean \pm SD) were used. See SI S4 for
 214 model scripts.
 215

216 The $\delta^{18}\text{O}_{\text{P}(\text{export})}$ range was first defined assuming no biological turnover prior to export (Eq. 2):

217 (Eq. 2)
$$\delta^{18}\text{O}_{\text{P}(\text{export.1})} = f_{\text{fert}}\delta^{18}\text{O}_{\text{P}(\text{fert})} + f_{\text{soil}}\delta^{18}\text{O}_{\text{P}(\text{soil})}$$

218
$$1 = f_{\text{fert}} + f_{\text{soil}}$$

219
$$f_{\text{fert}} = P_{\text{fert}}/P_{\text{soil}}$$

220 where f_{fert} and f_{soil} are the contribution of PO_4^{3-} from fertiliser and soil, respectively, and $\delta^{18}\text{O}_{\text{P}(\text{fert})}$
 221 and $\delta^{18}\text{O}_{\text{P}(\text{soil})}$ their isotopic composition; f_{fert} was estimated for each soil texture based on its
 222 leachable soil P content (P_{soil}) and the recommended fertiliser application amount (P_{fert}). Two P_{soil}
 223 scenarios were considered: scenario a (fast), where export occurs within ~ 1 day of application (P_{soil}
 224 = H_2O extractable PO_4^{3-}), and scenario b (slow), where export occurs gradually over a whole season
 225 ($P_{\text{soil}} = \text{H}_2\text{O} + \text{NaHCO}_3$ extractable PO_4^{3-} (Rupp et al., 2018)).

226 Next, scenarios a and b were rerun to consider biological P turnover pushing $\delta^{18}\text{O}_{\text{P}}$ values
 227 towards $\delta^{18}\text{O}_{\text{P}(\text{eq})}$, as per (Helfenstein et al., 2018):

228 (Eq. 3) $\delta^{18}O_{P(\text{export.2})} = X_P \cdot (\delta^{18}O_{P(\text{eq})} - \delta^{18}O_{P(\text{export.1})}) + \delta^{18}O_{P(\text{export.1})}$
229 where an exchange factor (X_P) defines $\delta^{18}O_{P(\text{export.1})}$ mixing with $\delta^{18}O_{P(\text{eq})}$ (Gross and Angert, 2015).
230 Eq. 3 constrains the effects of short-term (daily to monthly) biological P cycling, so $\delta^{18}O_{P(\text{eq})}$ was
231 defined based on diurnal variations in winter soil temperatures (Eq. 1). As X_P is challenging to
232 measure directly, values were approximated for each soil texture based on soil P mean residence
233 time, calculated as the log-log linear relationship between H₂O extractable PO₄³⁻ and PO₄³⁻ turnover
234 in <1 hr, or, 2) NaOH extractable PO₄³⁻ and PO₄³⁻ turnover in >1 hr – 3 months (Helfenstein et al.,
235 2020). For biologically active ‘fast’ export (scenario c), X_P was defined as PO₄³⁻ exchange in < 1 hr
236 and applied to scenario a $\delta^{18}O_{P(\text{export.1})}$ values. For biologically active ‘slow’ export (scenario d), X_P
237 was defined as the proportion of PO₄³⁻ exchange in 1 hr – 3 months and applied to scenario b
238 $\delta^{18}O_{P(\text{export.1})}$ values.

239 $\delta^{18}O_{P(\text{fert})}$ variability was parameterised two ways. First, models were run using the annual
240 differences in $\delta^{18}O_{P(\text{fert})}$ measured 2013-2017 for different fertiliser types (AG and SP, but not MAP
241 because only one year was sampled). Second, P_{fert} was varied to reflect the low, high, and median
242 fertiliser application rates recommended for each soil texture: 14, 58, 37 kg P ha⁻¹ (clay), 18, 37, 28
243 kg P ha⁻¹ (loam), and 9, 13, 11 kg P ha⁻¹ (sand) (Summers and Weaver, 2011). Application rates (kg
244 P ha⁻¹) were converted to concentrations ($\mu\text{g P g}^{-1}$) in the top 10 cm of soil (P_{fert}) using regional
245 pasture soil bulk density (Viscarra Rossel et al., 2014): 1.44 ± 0.2 kg ha⁻¹ (clay), 1.25 ± 0.2 kg ha⁻¹
246 (loam), and 1.33 ± 0.1 kg ha⁻¹ (sand). This model does not consider the complex soil chemical
247 processes affecting long-term fertiliser mobility, meaning fertiliser contributions to ‘slow’ export
248 scenarios (b, d) may be overestimated.

249 Variability in soil inputs was parameterised by solving each export scenario (a: fast, b: slow,
250 c: fast + turnover, d: slow + turnover) using the mean, mean+SD, and mean-SD of $\delta^{18}O_{P(\text{soil})}$ and
251 P_{soil} for each soil texture, as well as for $\delta^{18}O_{P(\text{eq})}$ (Henry and Wickham, 2020): f_{fert} was calculated for
252 each P_{soil} and P_{fert} combination, the minimum, mean-SD, mean, mean+SD, and maximum f_{fert} for
253 scenarios (a, b) × soil texture used to solve Eq. 2 for each fertiliser × manufacturing year, and then

254 $\delta^{18}\text{O}_{\text{P}(\text{export},1)}$ values used to solve Eq. 3 for scenario (c, d) \times soil texture for each fertiliser \times
255 manufacturing year (Fig. 1). Output $\delta^{18}\text{O}_{\text{P}(\text{export})}$ ranges were upscaled to possible ‘agricultural soil’
256 signatures based on the measured PO_4^{3-} content and spatial coverage of soil textures for two sub-
257 catchments with contrasting soil distributions, see SI Fig. S2 (McArthur and Bettenay, 1974; Weller,
258 2019). Upscaling calculations varied the contribution of AG v SP fertilisers and timing between
259 fertilisation and export (a: fast v d: slow + turnover).

260

261 3. Results

262 3.1 Fertilisers

263 Fertiliser types had different $\delta^{18}\text{O}_{\text{P}(\text{fert})}$ values ($p < 0.05$, $F = 52$). Values ranged from $17 \pm$
264 1 ‰ (SP) to $22 \pm 0.05 \text{ ‰}$ (MAP) (Table 2). The $\delta^{18}\text{O}_{\text{P}(\text{fert})}$ composition of SP and AG varied between
265 manufacturing years: SP from $16 \pm 0.2 \text{ ‰}$ in 2015 to $19 \pm 0.2 \text{ ‰}$ in 2013, and AG from $20 \pm 0.4 \text{ ‰}$
266 in 2014 to $22 \pm 0.01 \text{ ‰}$ in 2015.

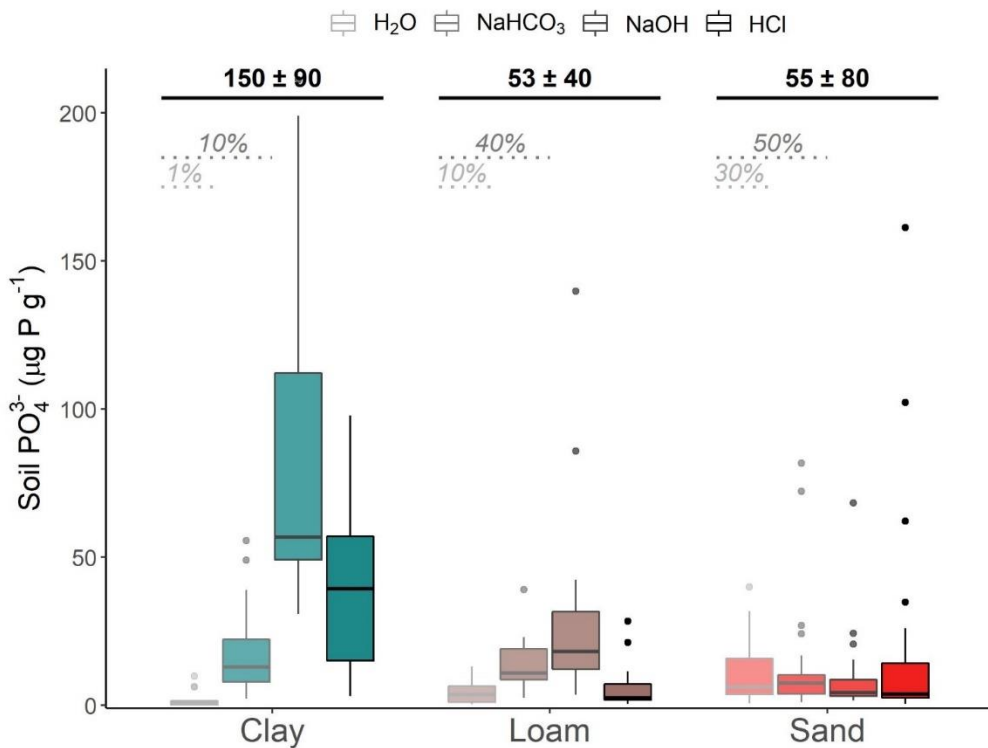
267

268 3.2 Soils

269 Soil pH was higher in clays than in loams or sands ($p < 0.05$, $F = 5.2$) (Table 1). C_{org} was higher
270 in clays ($66 \pm 20 \text{ mg C g}^{-1}$) than loams ($40 \pm 10 \text{ mg C g}^{-1}$) and sands ($38 \pm 30 \text{ mg C g}^{-1}$) ($F = 2.7$,
271 $p < 0.05$) (Table 1), as was P_{total} (clay: $360 \pm 20 \text{ } \mu\text{g g}^{-1}$, loam: $190 \pm 90 \text{ } \mu\text{g g}^{-1}$, sand: $120 \pm 100 \text{ } \mu\text{g g}^{-1}$)
272 ($F = 20$, $p < 0.05$). P_{org} did not differ between soil textures or farms (SI Table S1), so P_{org}
273 accounted for a higher proportion of P_{total} in sands ($57 \pm 10 \text{ %}$) than loams ($45 \pm 10 \text{ %}$) and clays
274 ($41 \pm 0.09 \text{ %}$) ($F = 12$, $p < 0.01$). The $\text{C}_{\text{org}}:\text{P}_{\text{org}}$ ratio was higher in sands ($630 \pm 500 \text{ g/g}$) than in clays
275 ($540 \pm 300 \text{ g/g}$) or loams ($530 \pm 200 \text{ g/g}$) ($F = 3.3$, $p < 0.01$; Table 1). $\text{P}_{\text{min(14)}}$ was highest in absolute
276 ($F = 10$, $p < 0.05$) terms in sands (SI Table S3), and decreased as a proportion of P_{TIP} from sands ($14 \pm 10 \text{ mg g}^{-1}$)
277 to loams ($4.4 \pm 3 \text{ mg g}^{-1}$) to clays ($0.74 \pm 0.4 \text{ mg g}^{-1}$) ($F = 23$, $p < 0.001$; Table 1).

278 P_{TIP} (based on $\text{H}_2\text{O}+\text{NaHCO}_3+\text{NaOH}+\text{HCl}$ fractions) was higher in clays ($150 \pm 90 \text{ } \mu\text{g P g}^{-1}$)
279 than loams ($53 \pm 50 \text{ } \mu\text{g P g}^{-1}$) or sands ($55 \pm 80 \text{ } \mu\text{g P g}^{-1}$) ($F = 11$, $p < 0.05$; Fig. 2). Water extractable

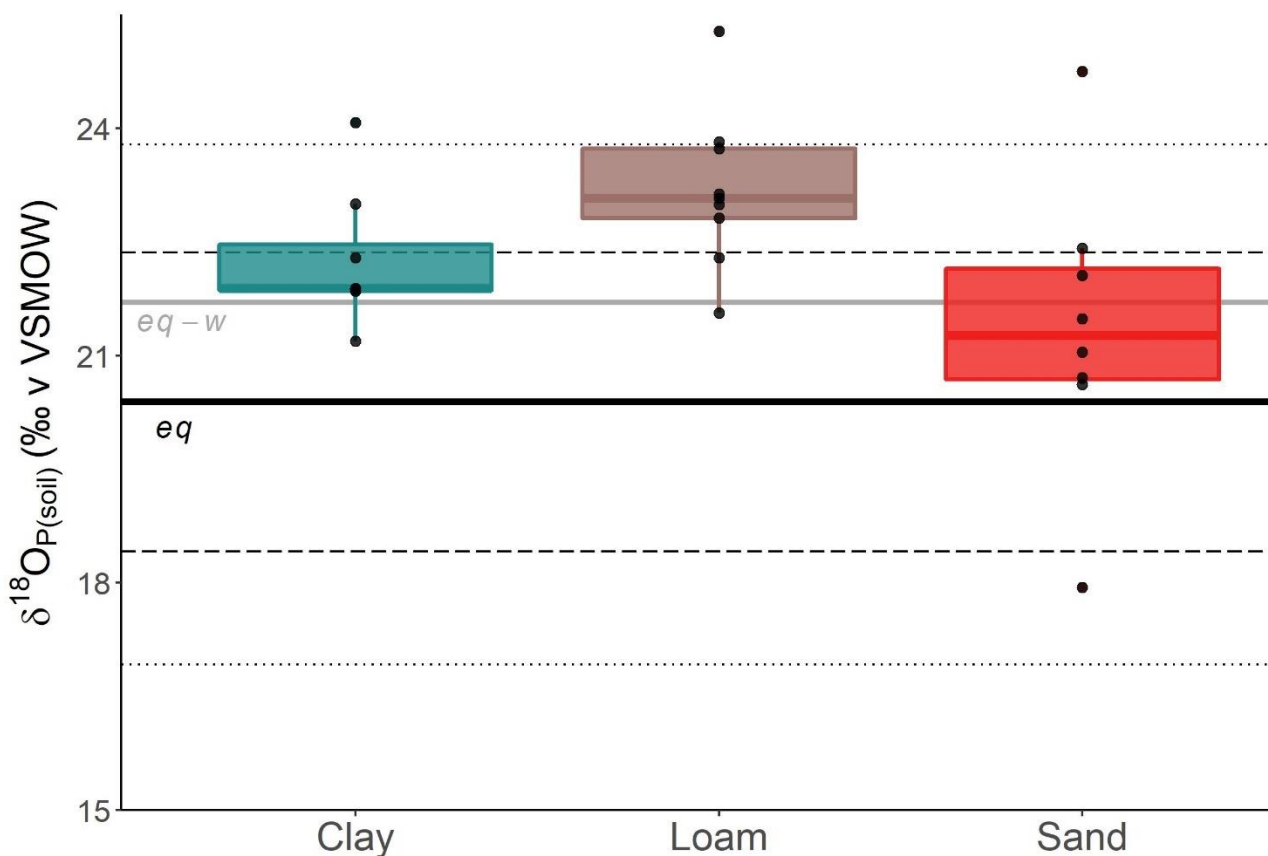
280 PO₄³⁻ differed between soil textures ($F = 9.6, p < 0.05$), with concentrations in sands ($11 \pm 10 \mu\text{g P g}^{-1}$)
 281 higher than in loams ($4.2 \pm 3 \mu\text{g P g}^{-1}$) and clays ($1.7 \pm 2 \mu\text{g P g}^{-1}$) (Fig. 2). NaHCO₃ extractable
 282 PO₄³⁻ did not differ between soil textures, but differed between farms ($F = 3.0, p = 0.019$): heavy
 283 clay soils in F6 had the lowest concentrations ($7.6 \pm 4 \mu\text{g P g}^{-1}$) and the predominantly sand soils in
 284 F1 had the highest ($27 \pm 20 \mu\text{g P g}^{-1}$) (see SI S2 for farm-level data). Clays had higher NaOH
 285 extractable PO₄³⁻ ($89 \pm 50 \mu\text{g P g}^{-1}$) than loams ($29 \pm 30 \mu\text{g P g}^{-1}$) or sands ($9.5 \pm 10 \mu\text{g P g}^{-1}$) ($F =$
 286 26, $p < 0.001$). Likewise, HCl extractable PO₄³⁻ was the highest in clays ($39 \pm 20 \mu\text{g P g}^{-1}$) and the
 287 lowest in loams ($6.0 \pm 8 \mu\text{g P g}^{-1}$) ($F = 3.9, p < 0.05$). 30% of P_{TIP} was H₂O extractable in sands,
 288 versus 10% in loams and 1% in clays ($F = 28, p < 0.001$; Fig. 2). The proportion of P_{TIP} in the
 289 H₂O+NaHCO₃ fraction also decreased from sands ($54 \pm 20 \%$) to loams ($41 \pm 20 \%$) to clays ($13 \pm$
 290 5%) ($F = 40, p < 0.001$; Fig. 2). X_P (Eq. 3) estimated for <1 hr was 30% (sand), 10% (loam), and 1%
 291 (clay), while X_P estimated for turnover >1 hr – 3 months was 20% (sand), 60% (loam), and 90%
 292 (clay), see SI Table S7.



293

294 **Fig. 2** Phosphate in surface soils (0 – 10 cm) of 21 pastures with different soil textures in the Peel-Harvey catchment
 295 (Western Australia) based on sequential extraction with H₂O (left, light outline), NaHCO₃, NaOH, and HCl (right, dark
 296 outline). P_{TIP} concentrations (sum of four fractions) for each soil textures is indicated at the top, and the percentage
 297 contribution of H₂O (easily leachable) and H₂O+NaHCO₃ (seasonally leachable) fractions indicated with dashed lines.
 298 Boxes represent median ± 1 SD.

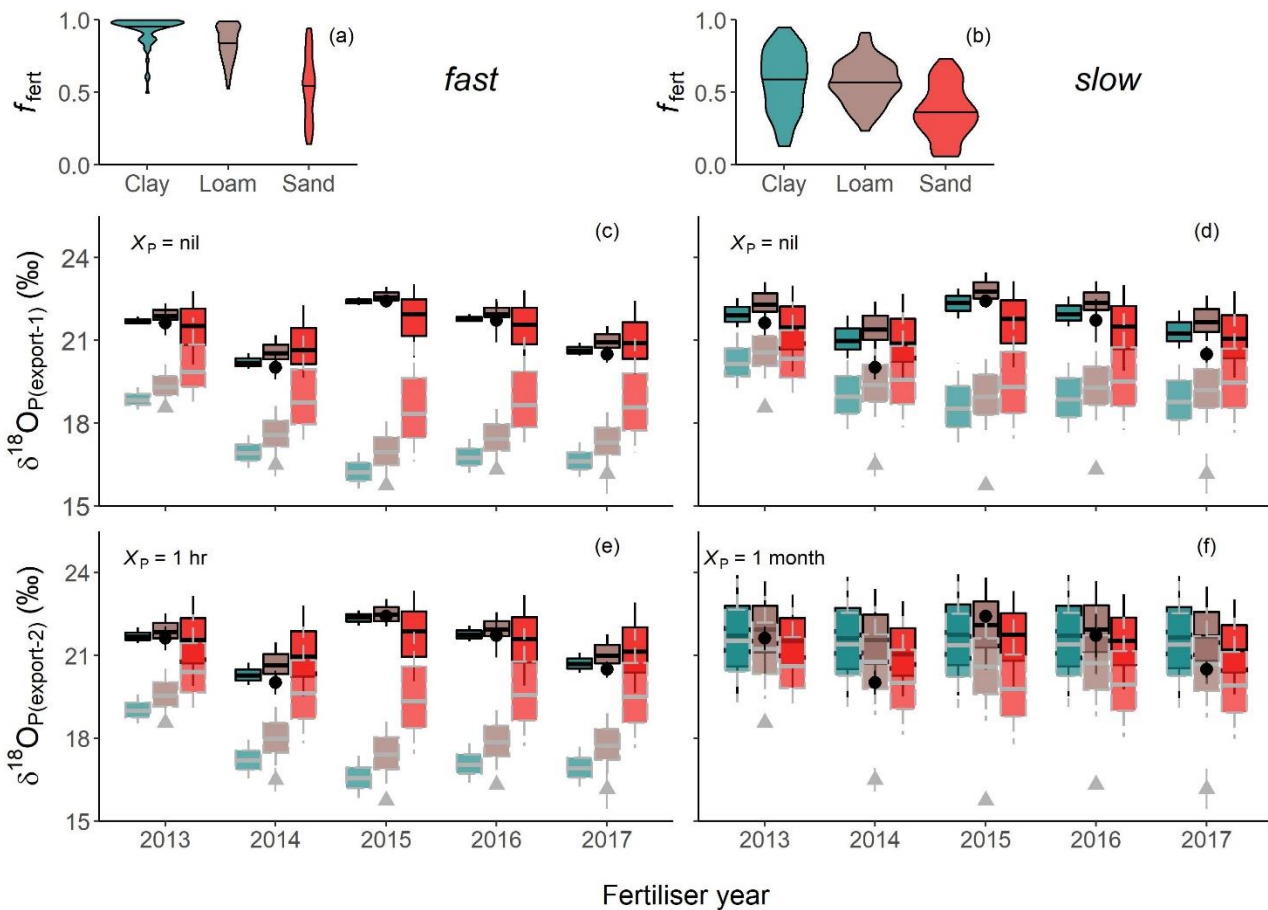
299 $\delta^{18}\text{O}_{\text{P}(\text{soil})}$ values ranged from 25.3‰ (F4 loam) to 17.9‰ (F2 sand). Values negatively
 300 correlated with $P_{\min(14)}$ ($p = 0.03$, $r = -0.45$) and positively correlated with C_{org} ($p = 0.03$, $r = 0.5$).
 301 Soil P concentrations did not correlate with $\delta^{18}\text{O}_{\text{P}(\text{soil})}$. $\delta^{18}\text{O}_{\text{P}(\text{soil})}$ values differed between soil
 302 textures but not farms, and were higher in loams (23.2 ± 1 ‰) than clays (22.3 ± 0.9 ‰) or sands
 303 (21.4 ± 2 ‰) ($p < 0.05$; $F = 3.8$; Fig. 3). $\delta^{18}\text{O}_{\text{P}(\text{eq})}$ values calculated using long-term temperature and
 304 $\delta^{18}\text{O}_{\text{H}_2\text{O}}$ records ranged from 16.9 to 23.8‰ (20.4 ± 1.97 ‰), versus from 19.3 – 24.1‰ based on
 305 winter soil temperatures and $\delta^{18}\text{O}_{\text{H}_2\text{O}}$ (Fig. 3). This places loam $\delta^{18}\text{O}_{\text{P}(\text{soil})}$ values at or above the
 306 maximum $\delta^{18}\text{O}_{\text{P}(\text{eq})}$ range, versus sand $\delta^{18}\text{O}_{\text{P}(\text{soil})}$ values around mean $\delta^{18}\text{O}_{\text{P}(\text{eq})}$.
 307



308
 309 **Fig. 3** The $\delta^{18}\text{O}_{\text{P}}$ of P_{TIP} in pasture soils (0–10 cm) classed as either clay, loam, or sand from six farms across the Peel-
 310 Harvey catchment (Western Australia). Boxes represent median ± 1 SD for each soil textures. Black lines represent the
 311 mean (solid line), ± 1 SD (dashed lines), and minimum/maximum (dotted lines) of the long-term local $\delta^{18}\text{O}_{\text{P}(\text{eq})}$ range
 312 (Eq. 2); the grey line indicates the mean $\delta^{18}\text{O}_{\text{P}(\text{eq})}$ calculated for conditions during the winter sampling ($eq-w$).
 313
 314

315 3.3 Export model

316 For scenario (a), f_{fert} (Eq. 2) decreased from 0.93 ± 0.1 (clays) via 0.84 ± 0.1 (loams) to 0.54
317 ± 0.2 (sands) (Fig. 4a). For scenario (b), f_{fert} was 0.57 ± 0.1 for clays, 0.57 ± 0.1 for loams, and 0.37
318 ± 0.2 for sands (Fig. 4b). In scenario (a) $\delta^{18}\text{O}_{\text{P}(\text{export})}$ values track $\delta^{18}\text{O}_{\text{P}(\text{fert})}$, with clear differences
319 between AG v SP applied to all soil textures (Fig. 4c). Rapid P turnover (scenario c) shifted sand,
320 but not clays or loams, $\delta^{18}\text{O}_{\text{P}(\text{export})}$ away from low-end $\delta^{18}\text{O}_{\text{P}(\text{fert})}$ values (Fig. 4e). Yearly $\delta^{18}\text{O}_{\text{P}(\text{fert})}$
321 differences in SP (2013 v 2014-2017) and AG (2014 v 2015) fertilisers affected modelled
322 $\delta^{18}\text{O}_{\text{P}(\text{export})}$ from clays and loams, but not sands, under ‘fast’ scenarios (a, c) (Fig. 4c,e). For ‘slow’
323 scenarios (b, d), differences in SP v AG $\delta^{18}\text{O}_{\text{P}(\text{export})}$ values were only expressed when $X_{\text{P}} = 0\%$ (Fig.
324 4d), and $\delta^{18}\text{O}_{\text{P}(\text{export})}$ from all soil textures and fertilisers normalised to $\delta^{18}\text{O}_{\text{P}(\text{eq})}$ with ~monthly P
325 turnover (Fig. 4f). Upscaling to sub-catchments, the possible $\delta^{18}\text{O}_{\text{P}(\text{export})}$ range is narrowest (~2‰)
326 if export is slow and fertilisation type uniform (Table 3). In both sub-catchments fertiliser mixing
327 was more important than the export speed in defining the $\delta^{18}\text{O}_{\text{P}(\text{export})}$ values, and mixed fertilisers +
328 slow export produced the widest possible $\delta^{18}\text{O}_{\text{P}(\text{export})}$ range.



329

330 **Fig. 4** The possible range of the isotopic composition of PO_4^{3-} export from clay, loam, and sand pasture soils
 331 ($\delta^{18}\text{O}_{\text{P}(\text{export})}$, ‰ v. VSMOW) within a catchment depends on fertiliser contribution to the leachable soil PO_4^{3-} pool (f_{fert})
 332 and fertiliser $\delta^{18}\text{O}_{\text{P}}$ composition (AG: black circles, SP: grey triangles, manufactured 2013–2017). $\delta^{18}\text{O}_{\text{P}(\text{export})}$ values
 333 were calculated for two export scenarios: fast (a, c, e), where PO_4^{3-} is exported <1 day after fertilisation, and slow (b, d,
 334 f), where PO_4^{3-} is leached over weeks-months. Both fast and slow export could occur with (e, f: $X_{\text{P}} = 1 \text{ h}$ or 1 month) or
 335 without (c, d: $X_{\text{P}} = \text{nil}$) soil biological P turnover (Eq. 3). Violins (a, b) show the distribution of f_{fert} values around the
 336 mean (solid line); boxes (c–f) show the mean $\pm 1 \text{ SD}$ for $\delta^{18}\text{O}_{\text{P}(\text{export})}$, with whiskers to the minimum and maximum. Box
 337 colours distinguish soil textures (as defined in a and b) and outlines the fertiliser (AG: black, SP: grey).

338

339

340 4. Discussion

341 4.1 Fertilisers

342 The $\delta^{18}\text{O}_{\text{P}(\text{fert})}$ range here (17 – 21 ‰) fits previous reports for inorganic commercial
 343 fertilisers (Table 2). Variations in $\delta^{18}\text{O}_{\text{P}(\text{fert})}$ are generally attributed to geologic differences in the
 344 rocks sourced to make the fertilisers (Davies et al., 2014; Gruau et al., 2005). This is because the
 345 $\delta^{18}\text{O}_{\text{P}}$ composition of the sedimentary rocks sourced to produce PO_4^{3-} fertilisers depend on age
 346 and/or equilibration with $\delta^{18}\text{O}_{\text{H}_2\text{O}}$ during formation (Sun et al., 2020). Here the ~8 ‰ difference
 347 between N-bearing (AG, MAP) and rock (SP) fertilisers corresponded with different geologic

348 source materials: AG and MAP were manufactured using materials from Florida, USA (Eocene –
349 Miocene, ~55 MBP (Trueman, 1965)), while SP was manufactured using Christmas Island rocks
350 (Oligocene – Pliocene, ~33 MBP (Van Kauwenbergh et al., 1990)). However, this explanation for
351 the 5 - 8 ‰ difference between the fertiliser types does not hold up to scrutiny. The ~20 MY gap is
352 negligible in geologic time (e.g., the 3 ‰ difference between PO_4^{3-} in China v the Middle East
353 corresponds to ~300 MY (Sun et al., 2020)). Likewise, different $\delta^{18}\text{O}_{\text{P(eq)}}$ during formation is
354 unlikely given similarities in the $\delta^{18}\text{O}_{\text{H}_2\text{O}}$ and temperature regimens between the Indian Ocean and
355 tropical Atlantic (LeGrande and Schmidt, 2006). This suggests that there is an additional factor than
356 the commonly cited ‘geologic $\delta^{18}\text{O}_{\text{P}}$ differences’ that is contributing to the consistent offset between
357 fertiliser types. We note that geology-driven variations in $\delta^{18}\text{O}_{\text{P(fert)}}$ is not robustly supported by the
358 literature, with source material origins provided in only four of nine published studies (Table 2).
359 This suggests that future work should encompass isotopic fractionation during manufacturing,
360 which is theoretically possible given the filtration and solubilisation processes used (Chien et al.,
361 2011), especially given the consistent differences between fertilisers made from raw (SP) v pre-
362 processed (AG, MAP) materials. A similar mechanism was proposed to explain differences in tap
363 water $\delta^{18}\text{O}_{\text{P}}$ (Goody et al., 2015), and requires further consideration.

364 Regardless of the exact driver (source, manufacturing), a single precise $\delta^{18}\text{O}_{\text{P(fert)}}$ value is
365 unlikely to exist at the spatial and temporal scale of catchment studies. Establishing methods for
366 predicting, and thus better constraining, $\delta^{18}\text{O}_{\text{P(fert)}}$ will be critical to any future attempts to use $\delta^{18}\text{O}_{\text{P}}$
367 to trace aquatic PO_4^{3-} . As first steps, we recommend future isotope studies report both the chemical
368 form and geologic (rather than commercial) origin of P fertilisers.

369

370 4.2 Soils

371 Soil P variations fit expectations (Table 1, Fig. 2). P_{TIP} content was at the very low end for
372 agricultural soils and $\text{C}_{\text{org}}:\text{P}_{\text{org}}$ ratios at the high end for mineral soils, both typical for weathered
373 southwestern Australian soils (Helfenstein et al., 2020; Spohn, 2020; Turner and Laliberte, 2015).

374 Phosphate partitioning followed the anticipated shift from sands with low, highly leachable, PO_4^{3-}
375 pools, to clays with larger, less leachable, PO_4^{3-} pools (Nash et al., 2019; O'Halloran et al., 1987).
376 These soil texture differences provide a solid basis to test how P buffering capacity controls
377 $\delta^{18}\text{O}_{\text{P(soil)}}$ and $\delta^{18}\text{O}_{\text{P(export)}}$.

378 $\delta^{18}\text{O}_{\text{P(soil)}}$ is hypothesised to reflect differences in the size and availability of soil PO_4^{3-}
379 (Bauke, 2020). Loosely bound PO_4^{3-} (H_2O or NaHCO_3 fractions) can be completely recycled in
380 days, whereas more tightly bound PO_4^{3-} (NaOH or HCl fractions) turnover may take centuries
381 (Helfenstein et al., 2020). Because biological PO_4^{3-} turnover moves $\delta^{18}\text{O}_{\text{P(soil)}}$ towards $\delta^{18}\text{O}_{\text{P(eq)}}$,
382 more labile PO_4^{3-} fractions tends to have (higher) $\delta^{18}\text{O}_{\text{P}}$ values closer to $\delta^{18}\text{O}_{\text{P(eq)}}$ and more tightly
383 bound PO_4^{3-} fractions tend to have (lower) $\delta^{18}\text{O}_{\text{P(soil)}}$ values closer to the geologic parent material
384 $\delta^{18}\text{O}_{\text{P}}$ (Roberts et al., 2015; Tian et al., 2020). This predicts that the sands' predominantly labile
385 PO_4^{3-} pool would shift $\delta^{18}\text{O}_{\text{P(soil)}}$ values higher than the clays, where most PO_4^{3-} is tightly bound
386 (Rodionov et al., 2020). Instead, the sands had the lowest $\delta^{18}\text{O}_{\text{P(soil)}}$ values, and almost all $\delta^{18}\text{O}_{\text{P(soil)}}$
387 values fell within the $\delta^{18}\text{O}_{\text{P(eq)}}$ range (Fig. 3). It is reasonable that all soil PO_4^{3-} was within the
388 $\delta^{18}\text{O}_{\text{P(eq)}}$ range as geologic PO_4^{3-} is unlikely to persist in any of these ~300,000 year old soils (Shen
389 et al., 2020; Turner and Laliberte, 2015). But if PO_4^{3-} is in isotopic equilibrium with soil water, why
390 do $\delta^{18}\text{O}_{\text{P(soil)}}$ values fall into distinct 'soil texture' zones within this range?

391 Variations within the $\delta^{18}\text{O}_{\text{P(eq)}}$ range could be driven by three factors: divergent equilibrium
392 conditions (soil temperature, $\delta^{18}\text{O}_{\text{H}_2\text{O}}$), different PO_4^{3-} sources, and/or fractionation by competing
393 biological processes. First, daily – seasonal parameter fluctuations are not seen to affect $\delta^{18}\text{O}_{\text{P(soil)}}$ of
394 P_{TIP} (Angert et al., 2011; Lei et al., 2019). This suggests that long-term evaporation ($\delta^{18}\text{O}_{\text{H}_2\text{O}}$) or
395 temperature differences between the soil textures would be needed to create a 'soil specific'
396 $\delta^{18}\text{O}_{\text{P(eq)}}$ range. Factors like slope, aspect, and vegetation (Hacker et al., 2019; Sprenger et al., 2016)
397 are excluded here due to the flat terrain and relatively homogenous land-use, but soil texture can
398 affect evaporation. However, a textural impact on evaporation would elevate $\delta^{18}\text{O}_{\text{P(soil)}}$ in coarse
399 grained sands above $\delta^{18}\text{O}_{\text{P(soil)}}$ in the fine grained clays (Gazis and Feng, 2004), the opposite of the

400 observed pattern. Second, pastures receive P_{org} and PO₄³⁻ inputs. Inorganic fertilisers can be ruled
401 out as δ¹⁸O_{P(fert)} values were lower than loam δ¹⁸O_{P(soil)} (Fig. 4), and likewise processed P_{org}
402 (manure) likely has δ¹⁸O_P below the δ¹⁸O_{P(soil)} range here (Granger et al., 2017b). While raw P_{org}
403 inputs (plants) can have δ¹⁸O_P up to ~30 ‰ (Pfahler et al., 2013; von Sperber et al., 2015), the
404 mechanism through which they could differently affect soil textures under similar management
405 (including pasture plants) is unclear. Charred organic matter is also a potentially significant P input
406 (Baldock et al., 2013). A survey of nearby pastures suggests that loams contain more char than
407 sands or clays (9.2 ± 2 mg C g⁻¹ v 7.7 ± 2 mg C g⁻¹ and 4.9 ± 2 mg C g⁻¹, respectively) (Viscarra
408 Rossel et al., 2014). If char contains 20 µg PO₄³⁻·P g⁻¹ (Pluchon et al., 2015), this could be the
409 source of 30% of loam PO₄³⁻, v 5% of clay PO₄³⁻. This is an intriguing possibility, but
410 measurements of combusted organic material suggest char δ¹⁸O_P values may be too low (~15 ‰)
411 (Bigio and Angert, 2019) to explain the observed loam δ¹⁸O_{P(soil)} values.

412 Alternatively, both the mineralisation of P_{org} to PO₄³⁻ and microbial PO₄³⁻ assimilation affect
413 δ¹⁸O_P. Scavenging P_{org} in low fertility soils can decrease δ¹⁸O_{P(soil)} below δ¹⁸O_{P(eq)} (Liang and Blake,
414 2006; Pistocchi et al., 2020), and estimates suggest that mineralisation is highest (P_{min} = ~1% of
415 P_{TIP} per fortnight) in the P-poor, relatively low δ¹⁸O_{P(soil)} sands (Table 1). Additionally, microbial
416 PO₄³⁻ assimilation increases δ¹⁸O_{P(soil)} (Blake et al., 2005), with stronger fractionation when P is
417 limiting (Lis et al., 2019). This gives a plausible explanation for the relatively high loam δ¹⁸O_{P(soil)}
418 values. Low P in both sands and loams could promote microbial PO₄³⁻ uptake and increase δ¹⁸O_{P(soil)}
419 of both soil textures (Bünemann et al., 2012), but the low sand C_{org} and P content causes its
420 microbial P to be more efficiently recycled and δ¹⁸O_{P(soil)} reset to the mean δ¹⁸O_{P(eq)} range. This
421 supports the assumption in catchment models that sand PO₄³⁻ is completely exhausted every winter
422 (Summers et al., 1999). Although the exact driver of the soil textures δ¹⁸O_{P(soil)} patterns is not
423 certain, the non-random distribution of δ¹⁸O_{P(soil)} within the δ¹⁸O_{P(eq)} range emphasises the need to
424 move beyond simply defining δ¹⁸O_{P(soil)} as ‘in’ or ‘out’ of equilibrium and start unpicking the
425 competing biological and hydrologic processes at play.

426

427 4.3 $\delta^{18}\text{O}_\text{P}$ as a tracer of PO_4^{3-} export from agricultural systems

428 There are three main questions about agricultural P export that $\delta^{18}\text{O}_\text{P}$ models look to answer:

429 1) how much fertiliser is exported directly to water?, 2) which landscape units contribute

430 disproportionately to PO_4^{3-} export?, and, 3) how much does agriculture contribute to catchment

431 PO_4^{3-} loads? The mixing models used here generated clear constraints on how $\delta^{18}\text{O}_\text{P}$ data could be

432 used at each of these scales.

433 Directly exported P fertilisers are a significant financial and environmental risk. Although

434 difficult to measure, estimates suggest fertilisers account for 30-80% of PO_4^{3-} leached from

435 agricultural systems (Nash et al., 2019), and radiotracer studies show 20-30 % of fertiliser PO_4^{3-} is

436 leached from pastures within two months of application (McLaren et al., 2017; McLaren et al.,

437 2016). There is further uncertainty about the timing of these direct export events: how long

438 fertilisers stay in granular form depends on rainfall, temperature, and fertiliser type (McLaren et al.,

439 2017). The wide $\delta^{18}\text{O}_{\text{P}(\text{fert})}$ range reported here indicates that $\delta^{18}\text{O}_\text{P}$ values could prove a uniquely

440 powerful tool for untangling these PO_4^{3-} leaching dynamics at the plot - paddock scale if

441 isotopically distinct fertiliser v soils were first identified. Yet the same $\delta^{18}\text{O}_{\text{P}(\text{fert})}$ range complicates

442 efforts to identify soil and land-use specific $\delta^{18}\text{O}_{\text{P}(\text{export})}$ signatures (Fig. 4, Table 3).

443 The twin possibilities of mixed fertiliser use and variable biological P turnover drive the

444 uncertainty in $\delta^{18}\text{O}_{\text{P}(\text{export})}$. Across the modelled two sub-catchments the ‘agricultural’ $\delta^{18}\text{O}_{\text{P}(\text{export})}$

445 could reasonably range between 18‰ and 25‰, a much wider range than would be predicted by

446 simply using the sub-catchment soil maps to upscale $\delta^{18}\text{O}_{\text{P}(\text{soil})}$. This level of uncertainty means

447 large datasets of receiving water $\delta^{18}\text{O}_\text{P}$ values are needed to generate statistically robust

448 identification of the fertiliser and soil PO_4^{3-} sources. For instance, measuring an ‘out of equilibrium’

449 downstream $\delta^{18}\text{O}_\text{P}$ value of 19‰ could reasonably be evidence of SP export, but would not rule out

450 export of other fertilisers contributing up to 40% of PO_4^{3-} . Conversely, measuring a $\delta^{18}\text{O}_\text{P}$ value of

451 21‰, well above the SP $\delta^{18}\text{O}_{\text{P}(\text{fert})}$ range, could not conclusively rule SP out as a PO_4^{3-} source (Fig.

452 4, Table 3). So while biological P turnover could ameliorate some of the variability created by
453 fertiliser-soil mixing by shifting $\delta^{18}\text{O}_{\text{P}(\text{export})}$ values towards $\delta^{18}\text{O}_{\text{P}(\text{eq})}$, it also highlights more
454 intransigent sources of uncertainty. First, the soil $\delta^{18}\text{O}_{\text{P}(\text{eq})}$ range is itself uncertain due to questions
455 around the extent to which variations are caused by hydrology (temperature and $\delta^{18}\text{O}_{\text{H}_2\text{O}}$ (Benettin
456 et al., 2018; Skrzypek et al., 2019)) v biology (balance between biological P cycling pathways
457 (Helfenstein et al., 2018; Siegenthaler et al., 2020)). Second, evaluating these questions about soil
458 $\delta^{18}\text{O}_{\text{P}(\text{eq})}$ dynamics is complicated by the fact that the PO_4^{3-} pools that can be extracted for $\delta^{18}\text{O}_{\text{P}}$
459 analysis do not necessarily align with those that are environmentally relevant (Gu and Margenot,
460 2020; McConnell et al., 2020). Both situations contrast with the established approaches to tracing
461 PO_4^{3-} pollution point sources like wastewater effluent (Goddy et al., 2018), where biological
462 modification of the defined source signature will occur post export to the waterway (Davies et al.,
463 2014). The interconnected uncertainties about P turnover and $\delta^{18}\text{O}_{\text{P}(\text{eq})}$ must be resolved in order to
464 usefully incorporate $\delta^{18}\text{O}_{\text{P}}$ into P reactive transport models (Dorioz et al., 1998). One potential is
465 that improved $\delta^{18}\text{O}_{\text{P}(\text{eq})}$ understanding could be used to construct $\delta^{18}\text{O}_{\text{P}}$ catchment models based on
466 temperature and $\delta^{18}\text{O}_{\text{H}_2\text{O}}$ regimens.

467

468 5. Conclusions

469 The ability of phosphate isotopes ($\delta^{18}\text{O}_{\text{P}}$) to trace diffuse agricultural pollutants through
470 catchments is limited by variations in soil zone inputs and reactions. The analytical template here
471 highlights the importance, but also the limitations, of using site-specific $\delta^{18}\text{O}_{\text{P}(\text{fert})}$ values to identify
472 diffuse agricultural pollution. Uncertainty from $\delta^{18}\text{O}_{\text{P}}$ can reasonably be constrained via site-
473 specific measurements in smaller catchments, but until biological turnover (fractionation and rates)
474 is better defined surface water $\delta^{18}\text{O}_{\text{P}}$ signatures should be attributed to diffuse catchment sources
475 with caution.

476

477 **Associated content:** The Supporting Information pdf contains additional: S1) site maps (Figure S1:
478 Site map with farm locations, Figure S2: Sub-catchment maps with soil textures), S2) additional
479 soil data (Table S1: Background data on soil P status and N content, Table S2: Sequential extraction
480 soil PO_4^{3-} concentration information by farm \times soil texture, Table S3: $\text{P}_{\min(14)}$ data), S3) input
481 variables for $\delta^{18}\text{O}_{\text{P(eq)}}$ and mixing model calculations (Table S4: precipitation $\delta^{18}\text{O}_{\text{H}_2\text{O}}$ for winter
482 2017, Table S5: Long-term soil temperature data, Table S6: Modelled daily winter soil
483 temperatures, Table S7: Estimated P turnover (X_{P}) by soil texture), and, S4) R scripts (S4.1: $\delta^{18}\text{O}_{\text{P(eq)}}$
484 calculations, S4.2: mixing models, S4.3: up-scaling calculations). Soil data are available on
485 <https://figshare.com/s/e1416e6217fe0e7f3b10> (*link for review only, will be published with DOI
486 upon acceptance*).

487

488 **Acknowledgements:** Iain Alexander and Natasha Carlson-Perret (Southern Cross University)
489 assisted with soil P extractions. Robert Summers (Department of Primary Industries and Regional
490 Development, Western Australia) supplied background site data, soil sampling equipment, and
491 fertiliser samples. Fiona Valesini (Murdoch University) helped organise field work and secure
492 research funding. Thanks to Justin Mercy (CSBP) for information on fertiliser sources and
493 production, and to the six land owners for granting access to their properties. Research was funded
494 by Australian Research Council grant LP150100451 and by the UK's Natural Environment
495 Research Council Environmental Isotope Facility grant IP-1664-1116.

496

497 **Author contributions:** NSW, MYR, and BDE designed the study. NSW and MYR carried out the
498 study. PJW and ACS carried out isotopic extractions and analysed the samples. NSW and DCG
499 analysed the data. NSW and DCG wrote the manuscript, with input from all co-authors.

500

501

502

503 **References**

- 504 Achat, D.L., Bakker, M.R., Zeller, B., Pellerin, S., Bienaimé, S., Morel, C., 2010. Long-term
505 organic phosphorus mineralization in Spodosols under forests and its relation to carbon and
506 nitrogen mineralization. *Soil Biol. Biochem.* 42, 1479-1490.
- 507 Angert, A., Weiner, T., Mazeh, S., Tamburini, F., Frossard, E., Bernasconi, S.M., Sternberg, M.,
508 2011. Seasonal variability of soil phosphate stable oxygen isotopes in rainfall manipulation
509 experiments. *Geochim. Cosmochim. Acta* 75, 4216-4227.
- 510 Baldock, J.A., Sanderman, J., Macdonald, L.M., Puccini, A., Hawke, B., Szarvas, S., McGowan, J.,
511 2013. Quantifying the allocation of soil organic carbon to biologically significant fractions. *Soil*
512 *Res.* 51, 561-576.
- 513 Bauke, S.L., 2020. Game changer in soil science: Perspectives from the Fritz-Scheffer awardee.
514 Oxygen isotopes in phosphate-The key to phosphorus tracing? *J. Plant Nutr. Soil Sci.*, 8.
- 515 Benettin, P., Volkmann, T.H.M., von Freyberg, J., Frentress, J., Penna, D., Dawson, T.E., Kirchner,
516 J., 2018. Effects of climatic seasonality on the isotopic composition of evaporating soil waters.
517 *Hydrol. Earth Syst. Sci.* 22, 2881-2890.
- 518 Beusen, A.H.W., Bouwman, A.F., Van Beek, L.P.H., Mogollon, J.M., Middelburg, J.J., 2016.
519 Global riverine N and P transport to ocean increased during the 20th century despite increased
520 retention along the aquatic continuum. *Biogeosci.* 13, 2441-2451.
- 521 Bigio, L., Angert, A., 2019. Oxygen isotope signatures of phosphate in wildfire ash. *ACS Earth*
522 *Space Chem.* 3, 760-769.
- 523 Blake, R.E., O'Neil, J.R., Surkov, A.V., 2005. Biogeochemical cycling of phosphorus: Insights from
524 oxygen isotope effects of phosphoenzymes. *American Journal of Science* 305, 596-620.
- 525 Bolland, M.D.A., Allen, D.G., 1998. Spatial variation of soil test phosphorus and potassium,
526 oxalate-extractable iron and aluminum, phosphorus-retention index, and organic carbon content in
527 soils of Western Australia. *Commun. Soil Sci. Plant Anal.* 29, 381-392.
- 528 Bünenmann, E.K., Oberson, A., Liebisch, F., Keller, F., Annaheim, K.E., Huguenin-Elie, O.,
529 Frossard, E., 2012. Rapid microbial phosphorus immobilization dominates gross phosphorus fluxes
530 in a grassland soil with low inorganic phosphorus availability. *Soil Biol. Biochem.* 51, 84-95.
- 531 Chang, S.J., Blake, R.E., 2015. Precise calibration of equilibrium oxygen isotope fractionations
532 between dissolved phosphate and water from 3 to 37 degrees C. *Geochim. Cosmochim. Acta* 150,
533 314-329.
- 534 Chien, S.H., Prochnow, L.I., Tu, S., Snyder, C.S., 2011. Agronomic and environmental aspects of
535 phosphate fertilizers varying in source and solubility: an update review. *Nutr. Cycl. Agroecosys.* 89,
536 229-255.
- 537 Davies, C.L., Surridge, B.W.J., Goody, D.C., 2014. Phosphate oxygen isotopes within aquatic
538 ecosystems: Global data synthesis and future research priorities. *Sci. Total Environ.* 496, 563-575.
- 539 Dorioz, J.M., Cassell, E.A., Orand, A., Eisenman, K.G., 1998. Phosphorus storage, transport and
540 export dynamics in the Foron River watershed. *Hydrol. Process.* 12, 285-309.
- 541 Gazis, C., Feng, X.H., 2004. A stable isotope study of soil water: evidence for mixing and
542 preferential flow paths. *Geoderma* 119, 97-111.
- 543 Goody, D.C., Bowes, M.J., Lapworth, D.J., Lamb, A.L., Williams, P.J., Newton, R.J., Davies,
544 C.L., Surridge, B.W.J., 2018. Evaluating the stable isotopic composition of phosphate oxygen as a
545 tracer of phosphorus from waste water treatment works. *Appl. Geochem.* 95, 139-146.
- 546 Goody, D.C., Lapworth, D.J., Ascott, M.J., Bennett, S.A., Heaton, T.H.E., Surridge, B.W.J., 2015.
547 Isotopic fingerprint for phosphorus in drinking water supplies. *Environ. Sci. Technol.* 49, 9020-
548 9028.
- 549 Goody, D.C., Lapworth, D.J., Bennett, S.A., Heaton, T.H.E., Williams, P.J., Surridge, B.W.J.,
550 2016. A multi-stable isotope framework to understand eutrophication in aquatic ecosystems. *Water*
551 *Res.* 88, 623-633.

- 552 Granger, S.J., Harris, P., Peukert, S., Guo, R., Tamburini, F., Blackwell, M.S.A., Howden, N.J.K.,
553 McGrath, S., 2017a. Phosphate stable oxygen isotope variability within a temperate agricultural
554 soil. *Geoderma* 285, 64-75.
- 555 Granger, S.J., Heaton, T.H.E., Pfahler, V., Blackwell, M.S.A., Yuan, H.M., Collins, A.L., 2017b.
556 The oxygen isotopic composition of phosphate in river water and its potential sources in the Upper
557 River Taw catchment, UK. *Sci. Total Environ.* 574, 680-690.
- 558 Gross, A., Angert, A., 2015. What processes control the oxygen isotopes of soil bio-available
559 phosphate? *Geochim. Cosmochim. Acta* 159, 100-111.
- 560 Gruau, G., Legeas, M., Riou, C., Gallacier, E., ois Martineau, F., Henin, O., 2005. The oxygen
561 isotope composition of dissolved anthropogenic phosphates: a new tool for eutrophication research?
562 *Water Res.* 39, 232-238.
- 563 Gu, C., Margenot, A.J., 2020. Navigating limitations and opportunities of soil phosphorus
564 fractionation. *Plant Soil.*
- 565 Hacker, N., Wilcke, W., Oelmann, Y., 2019. The oxygen isotope composition of bioavailable
566 phosphate in soil reflects the oxygen isotope composition in soil water driven by plant diversity
567 effects on evaporation. *Geochim. Cosmochim. Acta* 248, 387-399.
- 568 Haygarth, P.M., Condron, L.M., Heathwaite, A.L., Turner, B.L., Harris, G.P., 2005. The
569 phosphorus transfer continuum: Linking source to impact with an interdisciplinary and multi-scaled
570 approach. *Sci. Total Environ.* 344, 5-14.
- 571 Hedley, M.J., Stewart, J.W.B., Chauhan, B.S., 1982. Changes in inorganic and organic soil
572 phosphorus fractions induced by cultivation practices and by laboratory incubations. *Soil Sci. Soc.*
573 *Am. J.* 46, 970-976.
- 574 Helfenstein, J., Pistocchi, C., Oberson, A., Tamburini, F., Goll, D.S., Frossard, E., 2020. Estimates
575 of mean residence times of phosphorus in commonly considered inorganic soil phosphorus pools.
576 *Biogeosci.* 17, 441-454.
- 577 Helfenstein, J., Tamburini, F., von Sperber, C., Massey, M.S., Pistocchi, C., Chadwick, O.A.,
578 Vitousek, P.M., Kretzschmar, R., Frossard, E., 2018. Combining spectroscopic and isotopic
579 techniques gives a dynamic view of phosphorus cycling in soil. *Nat. Commun.* 9, 9.
- 580 Henry, L., Wickham, H., 2020. purrr: Functional Programming Tools, R package version 0.3.4.,
581 <https://CRAN.R-project.org/package=purrr>.
- 582 Hollins, S.E., Hughes, C.E., Crawford, J., Cendón, D.I., Meredith, K.T., 2018. Rainfall isotope
583 variations over the Australian continent – Implications for hydrology and isoscape applications. *Sci.*
584 *Total Environ.* 645, 630-645.
- 585 IAEA/WMO, 2020. Global Network of Isotopes in Precipitation.
- 586 Ishida, T., Uehara, Y., Iwata, T., Cid-Andres, A.P., Asano, S., Ikeya, T., Osaka, K., Ide, J.,
587 Privaldos, O.L.A., De Jesus, I.B.B., Peralta, E.M., Trino, E.M.C., Ko, C.Y., Paytan, A., Tayasu, I.,
588 Okuda, N., 2019. Identification of phosphorus sources in a watershed using a phosphate oxygen
589 isoscape approach. *Environ. Sci. Technol.* 53, 4707-4716.
- 590 Jaisi, D.P., Kukkadapu, R.K., Stout, L.M., Varga, T., Blake, R.E., 2011. Biotic and abiotic
591 pathways of phosphorus cycling in minerals and sediments: Insights from oxygen isotope ratios in
592 phosphate. *Environ. Sci. Technol.* 45, 6254-6261.
- 593 Jensen, J.L., Christensen, B.T., Schjønning, P., Watts, C.W., Munkholm, L.J., 2018. Converting
594 loss-on-ignition to organic carbon content in arable topsoil: pitfalls and proposed procedure. *Eur. J.*
595 *Soil Sci.* 69, 604-612.
- 596 Kassambara, A., 2020. rstatix: Pipe-Friendly Framework for Basic Statistical Tests, R package
597 version 0.5.0 ed, <https://CRAN.R-project.org/package=rstatix>.
- 598 Kearney, M.R., 2019. MicroclimOz – A microclimate data set for Australia, with example
599 applications. *Austral Ecol.* 44, 534-544.
- 600 LeGrande, A.N., Schmidt, G.A., 2006. Global gridded data set of the oxygen isotopic composition
601 in seawater. *Geophys. Res. Lett.* 33, 5.

- 602 Lei, X.T., Chen, M., Guo, L.D., Zhang, X.G., Jiang, Z.H., Chen, Z.G., 2019. Diurnal variations in
603 the content and oxygen isotope composition of phosphate pools in a subtropical agriculture soil.
604 Geoderma 337, 863-870.
- 605 Li, X., Wang, Y., Stern, J., Cu, B.H., 2011. Isotopic evidence for the source and fate of phosphorus
606 in Everglades wetland ecosystems. Appl. Geochem. 26, 688-695.
- 607 Liang, Y., Blake, R.E., 2006. Oxygen isotope signature of P-i regeneration from organic
608 compounds by phosphomonoesterases and photooxidation. Geochim. Cosmochim. Acta 70, 3957-
609 3969.
- 610 Lis, H., Weiner, T., Pitt, F.D., Keren, N., Angert, A., 2019. Phosphate uptake by cyanobacteria is
611 associated with kinetic fractionation of phosphate oxygen isotopes. ACS Earth Space Chem. 3, 233-
612 239.
- 613 McArthur, W.M., Bettenay, E., 1974. The development and distribution of the soils of the Swan
614 Coastal Plain, Western Australia, 2nd ed. CSIRO, Melbourne, Australia.
- 615 McConnell, C.A., Kaye, J.P., Kemanian, A.R., 2020. Reviews and syntheses: Ironing out wrinkles
616 in the soil phosphorus cycling paradigm. Biogeoosci. 17, 5309-5333.
- 617 McLaren, T.I., McBeath, T.M., Simpson, R.J., Richardson, A.E., Stefanski, A., Guppy, C.N.,
618 Smernik, R.J., Rivers, C., Johnston, C., McLaughlin, M.J., 2017. Direct recovery of P-33-labelled
619 fertiliser phosphorus in subterranean clover (*Trifolium subterraneum*) pastures under field
620 conditions - The role of agronomic management. Agric. Ecosyst. Environ. 246, 144-156.
- 621 McLaren, T.I., McLaughlin, M.J., McBeath, T.M., Simpson, R.J., Smernik, R.J., Guppy, C.N.,
622 Richardson, A.E., 2016. The fate of fertiliser P in soil under pasture and uptake by subterraneum
623 clover - a field study using P-33-labelled single superphosphate. Plant Soil 401, 23-38.
- 624 McLaughlin, K., Cade-Menun, B.J., Paytan, A., 2006. The oxygen isotopic composition of
625 phosphate in Elkhorn Slough, California: A tracer for phosphate sources. Estuar. Coast. Shelf Sci.
626 70, 499-506.
- 627 Melland, A.R., Fenton, O., Jordan, P., 2018. Effects of agricultural land management changes on
628 surface water quality: A review of meso-scale catchment research. Environ. Sci. Policy 84, 19-25.
- 629 Metson, G.S., Lin, J.J., Harrison, J.A., Compton, J.E., 2017. Linking terrestrial phosphorus inputs to
630 riverine export across the United States. Water Res. 124, 177-191.
- 631 Nash, D.M., McDowell, R.W., Condron, L.M., McLaughlin, M.J., 2019. Direct exports of
632 phosphorus from fertilizers applied to grazed pastures. J. Environ. Qual. 48, 1380-1396.
- 633 O'Halloran, I.P., Stewart, J.W.B., Kachanoski, R.G., 1987. Influence of texture and management
634 practices on the forms and distribution of soil phosphorus. Can. J. Soil Sci. 67, 147-163.
- 635 Paytan, A., Roberts, K., Watson, S., Peek, S., Chuang, P.C., Defforey, D., Kendall, C., 2017.
636 Internal loading of phosphate in Lake Erie Central Basin. Sci. Total Environ. 579, 1356-1365.
- 637 Pedersen, T.L., 2019. patchwork: The Composer of Plots, R package version 1.0.0 ed,
638 <https://CRAN.R-project.org/package=patchwork>.
- 639 Pfahler, V., Durr-Auster, T., Tamburini, F., Bernasconi, S., Frossard, E., 2013. ^{18}O enrichment in
640 phosphorus pools extracted from soybean leaves. New Phytol. 197, 186-193.
- 641 Pistocchi, C., Meszaros, E., Frossard, E., Bunemann, E.K., Tamburini, F., 2020. In or out of
642 equilibrium? How microbial activity controls the oxygen isotopic composition of phosphate in
643 forest organic horizons with low and high phosphorus availability. Front. Environ. Sci. 8, 15.
- 644 Pistocchi, C., Tamburini, F., Gruau, G., Ferhi, A., Trevisan, D., Dorioz, J.M., 2017. Tracing the
645 sources and cycling of phosphorus in river sediments using oxygen isotopes: Methodological
646 adaptations and first results from a case study in France. Water Res. 111, 346-356.
- 647 Pluchon, N., Casetou, S.C., Kardol, P., Gundale, M.J., Nilsson, M.C., Wardle, D.A., 2015.
648 Influence of species identity and charring conditions on fire-derived charcoal traits. Can. J. For.
649 Res. 45, 1669-1675.
- 650 Polain, K., Guppy, C., Knox, O., Lisle, L., Wilson, B., Osanai, Y., Siebers, N., 2018. Determination
651 of agricultural impact on soil microbial activity using delta O-18(p) (HCl) and respiration
652 experiments. ACS Earth Space Chem. 2, 683-691.

- 653 Rivers, M.R., Weaver, D.M., Smettem, K.R.J., Davies, P.M., 2013. Estimating farm to catchment
654 nutrient fluxes using dynamic simulation modelling – Can agri-environmental BMPs really do the
655 job? *J Environ Manage* 130, 313-323.
- 656 Roberts, K., Defforey, D., Turner, B.L., Condron, L.M., Peek, S., Silva, S., Kendall, C., Paytan, A.,
657 2015. Oxygen isotopes of phosphate and soil phosphorus cycling across a 6500 year
658 chronosequence under lowland temperate rainforest. *Geoderma* 257–258, 14-21.
- 659 Rodionov, A., Bauke, S.L., von Sperber, C., Hoeschen, C., Kandeler, E., Kruse, J., Lewandowski,
660 H., Marhan, S., Mueller, C.W., Simon, M., Tamburini, F., Uhlig, D., von Blanckenburg, F., Lang,
661 F.D., Amelung, W., 2020. Biogeochemical cycling of phosphorus in subsoils of temperate forest
662 ecosystems. *Biogeochem.* 150, 313-328.
- 663 Rupp, H., Meissner, R., Leinweber, P., 2018. Plant available phosphorus in soil as predictor for the
664 leaching potential: Insights from long-term lysimeter studies. *Ambio* 47, 103-113.
- 665 Saunders, W.M.H., Williams, E.G., 1955. Observations on the determination of total organic
666 phosphorus in soils. *J. Soil Sci.* 6, 254-267.
- 667 Shen, J., Smith, A.C., Claire, M.W., Zerkle, A.L., 2020. Unraveling biogeochemical phosphorus
668 dynamics in hyperarid Mars-analogue soils using stable oxygen isotopes in phosphate. *Geobiology*
669 18, 760-779.
- 670 Siegenthaler, M.B., Tamburini, F., Frossard, E., Chadwick, O., Vitousek, P., Pistocchi, C.,
671 Meszaros, V., Helfenstein, J., 2020. A dual isotopic (P-32 and O-18) incubation study to
672 disentangle mechanisms controlling phosphorus cycling in soils from a climatic gradient (Kohala,
673 Hawaii). *Soil Biol. Biochem.* 149, 12.
- 674 Skrzypek, G., Dogramaci, S., Page, G.F.M., Rouillard, A., Grierson, P.F., 2019. Unique stable
675 isotope signatures of large cyclonic events as a tracer of soil moisture dynamics in the semiarid
676 subtropics. *J. Hydrol.* 578, 13.
- 677 Spohn, M., 2020. Increasing the organic carbon stocks in mineral soils sequesters large amounts of
678 phosphorus. *Global Change Biol.* 26, 4169-4177.
- 679 Sprenger, M., Leistert, H., Gimbel, K., Weiler, M., 2016. Illuminating hydrological processes at the
680 soil-vegetation-atmosphere interface with water stable isotopes. *Rev. Geophys.* 54, 674-704.
- 681 Sprenger, M., Tetzlaff, D., Soulsby, C., 2017. Soil water stable isotopes reveal evaporation
682 dynamics at the soil-plant-atmosphere interface of the critical zone. *Hydrol. Earth Syst. Sci.* 21,
683 3839-3858.
- 684 Summers, R.N., Van Gool, D., Guise, N.R., Heady, G.J., Allen, T., 1999. The phosphorus content
685 in the run-off from the coastal catchment of the Peel Inlet and Harvey Estuary and its associations
686 with land characteristics. *Agric. Ecosyst. Environ.* 73, 271-279.
- 687 Summers, R.N., Weaver, D.M., 2011. Soil test and phosphorus rate for high rainfall clover pastures.
688 Bulletin 4829.
- 689 Sun, Y., Amelung, W., Wu, B., Haneklaus, S., Maekawa, M., Lucke, A., Schnug, E., Bol, R., 2020.
690 'Co-evolution' of uranium concentration and oxygen stable isotope in phosphate rocks. *Appl.
691 Geochem.* 114, 9.
- 692 Tamburini, F., Bernasconi, S.M., Angert, A., Weiner, T., Frossard, E., 2010. A method for the
693 analysis of the $\delta^{18}\text{O}$ of inorganic phosphate extracted from soils with HCl. *Eur. J. Soil Sci.* 61,
694 1025-1032.
- 695 Tian, L.Y., Guo, Q.J., Yu, G.R., Zhu, Y.G., Lang, Y.C., Wei, R.F., Hu, J., Yang, X.R., Ge, T.D.,
696 2020. Phosphorus fractions and oxygen isotope composition of inorganic phosphate in typical
697 agricultural soils. *Chemosphere* 239, 10.
- 698 Tonderski, K., Andersson, L., Lindstrom, G., St Cyr, R., Schonberg, R., Taubald, H., 2017.
699 Assessing the use of delta O-18 in phosphate as a tracer for catchment phosphorus sources. *Sci.
700 Total Environ.* 607, 1-10.
- 701 Trueman, N.A., 1965. The phosphate, volcanic and carbonate rocks of Christmas Island (Indian
702 Ocean). *Journal of the Geological Society of Australia* 12, 261-283.

- 703 Turner, B.L., Laliberte, E., 2015. Soil development and nutrient availability along a 2 million-year
704 coastal dune chronosequence under species-rich Mediterranean shrubland in southwestern
705 Australia. *Ecosystems* 18, 287-309.
- 706 Valesini, F.J., Hallett, C.S., Hipsey, M.R., Kilminster, K.L., Huang, P., Hennig, K., 2019. Chapter 7
707 - Peel-Harvey Estuary, Western Australia, in: Wolanski, E., Day, J.W., Elliott, M., Ramachandran,
708 R. (Eds.), *Coasts and Estuaries*. Elsevier, pp. 103-120.
- 709 Van Kauwenbergh, S.J., Cathcart, J.B., McClellan, G.H., 1990. Mineralogy and alteration of the
710 phosphate deposits of Florida : a detailed study of the mineralogy and chemistry of the phosphate
711 deposits of Florida, United States Geological Survey Bulletin.
- 712 Viscarra Rossel, R.A., Webster, R., Bui, E.N., Baldock, J., 2014. Baseline map of Australian soil
713 organic carbon stocks and their uncertainty., in: CSIRO (Ed.), Data Collection, v2 ed.
- 714 von Sperber, C., Tamburini, F., Brunner, B., Bernasconi, S.M., Frossard, E., 2015. The oxygen
715 isotope composition of phosphate released from phytic acid by the activity of wheat and *Aspergillus*
716 *niger* phytase. *Biogeosci.* 12, 4175-4184.
- 717 Wan, H., Liu, W.G., 2016. An isotope study (delta O-18 and delta D) of water movements on the
718 Loess Plateau of China in arid and semiarid climates. *Ecol. Eng.* 93, 226-233.
- 719 Wang, Y., Bauke, S.L., von Sperber, C., Tamburini, F., Guigue, J., Winkler, P., Kaiser, K.,
720 Honermeier, B., Amelung, W., 2021. Soil phosphorus cycling is modified by carbon and nitrogen
721 fertilization in a long-term field experiment. *J. Plant Nutr. Soil Sci.* 184, 282-293.
- 722 Weller, H., 2019. countcolors: Locates and Counts Pixels Within Color Range(s) in Images, R
723 package version 0.9.1.
- 724 Wickham, C., 2018. munsell: Utilities for Using Munsell Colours, R package version 0.5.0,
725 <https://CRAN.R-project.org/package=munsell>.
- 726 Wickham, H., 2016. *ggplot2: Elegant Graphics for Data Analysis*. Springer-Verlag New York,
727 <https://ggplot2.tidyverse.org>.
- 728 Young, M.B., McLaughlin, K., Kendall, C., Stringfellow, W., Rollog, M., Elsbury, K., Donald, E.,
729 Paytan, A., 2009. Characterizing the oxygen isotopic composition of phosphate sources to aquatic
730 ecosystems. *Environ. Sci. Technol.* 43, 5190-5196.
- 731

732 **Tables**

733 **Table 1:** Characteristics of pasture soils (0 – 10 cm) with contrasting textures (sand, clay, loam) collected from six farms (F1 – F6) across the coastal
 734 Peel-Harvey catchment in southwestern Western Australia (see SI S1 maps). Sample numbers indicate the total bulked ($n = 3$) cores collected for P
 735 content and the subset analysed for $\delta^{18}\text{O}_{\text{P}(\text{soil})}$. The contribution of P_{org} to P_{total} is calculated on a g/g basis. Potential P mineralisation over 14 days
 736 ($\text{P}_{\text{min}(14)}$) is reported relative to the total HCl extractable PO_4^{3-} concentration (P_{TIP}). See SI S2 for additional soil chemistry data.

Texture	Farm	sample #s		pH	C_{org} <i>mg C g⁻¹</i>	P_{total} <i>µg P g⁻¹</i>	% P_{org} <i>($\text{P}_{\text{org}}/\text{P}_{\text{total}}$) · 100</i>	$\text{C}_{\text{org}}:\text{P}_{\text{org}}$ <i>g/g</i>	$\text{P}_{\text{min}(14)}:\text{P}_{\text{TIP}}$ <i>mg/g</i>
		<i>all</i>	$\delta^{18}\text{O}_{\text{P}}$						
Clay	F3	3	1	5.8 (0.1)	33	390 (70)	33 (9)	290 (100)	0.27 (0.07)
	F4	9	4	6.5 (0.3)	68 (20)	450 (200)	37 (7)	440 (100)	0.68 (0.3)
	F6	9	3	6.3 (0.1)	76 (20)	250 (60)	46 (7)	700 (300)	0.90 (0.4)
Loam	F2	6	4	6.1 (0.09)	34 (9)	150 (50)	41 (7)	590 (200)	6.6 (4)
	F4	3	2	6.4 (0.06)	58 (20)	320 (100)	37 (10)	540 (200)	1.9 (2)
	F5	9	3	6.3 (0.2)	38 (10)	170 (50)	51 (8)	490 (200)	3.9 (2)
Sand	F1	9	4	5.8 (0.3)	46 (40)	470 (600)	53 (10)	340 (200)	7.7 (7)
	F2	6	2	6.3 (0.09)	54 (30)	120 (80)	55 (10)	1000 (600)	18 (10)
	F3	9	2	6.2 (0.1)	16 (7)	63 (20)	61 (20)	510 (200)	16 (10)

737
738

739 **Table 2** Inorganic fertiliser $\delta^{18}\text{O}_\text{P}$ values reported for this study and others ($\delta^{18}\text{O}_{\text{P}(\text{fert})}$, values in ‰ v VSMOW), with respect to fertiliser type, where
 740 the fertiliser was manufactured, and where the PO_4^{3-} raw material was sourced from ('unspecified' denotes data unavailable).
 741

Fertiliser type	Manufactured	Sourced	$\delta^{18}\text{O}_{\text{P}(\text{fert})}$	Reference
Superphosphate	Australia	Christmas Island	16.7 ± 1 $15.6 - 18.7$	This study
	Europe	Unspecified	17.7 ± 0.2	Tamburini et al. (2010)
	Japan	Japan	12.7	Ishida et al. (2019)
	Australia	Unspecified	21.4 ± 0.5	Polain et al. (2018)
	Israel	Unspecified	21.8 ± 0.3	(Gross and Angert, 2015)
Monoammonium phosphate	Europe	Morocco & USA	23 ± 0.3	Gruau et al. (2005)
	Australia	USA	21.6 ± 0.05	This study
	Australia	Unspecified	20.2 ± 0.1	Polain et al. (2018)
N-P-S-K	Australia	USA	21.3 ± 1 $19.7 - 22.4$	This study
	Europe	Morocco & USA	21.8 ± 0.5	Gruau et al. (2005)
	Europe	Unspecified	20.9 ± 6	Granger et al. (2017b)
Unspecified	USA	USA	23.8 ± 1	Li et al. (2011)
	USA	Unspecified	19 ± 1	McLaughlin et al. (2006)
	USA	Israel	19.6	Young et al. (2009)
	China	China	11.5 ± 0.1	Tian et al. (2020)

742

743
744

745 **Table 3** Possible $\delta^{18}\text{O}_{\text{P}(\text{export})}$ range from two sub-catchments with differing soil distributions (maps:
 746 SI S1). The $\delta^{18}\text{O}_{\text{P}(\text{export})}$ range was calculated by varying the relative proportion of SP v AG
 747 fertilisers and speed of PO_4^{3-} transport from soil to water (fast, scenario a: mixing with H_2O
 748 extractable PO_4^{3-} pool, $X_{\text{P}} = 0\%$; or scenario d: mixing with $\text{H}_2\text{O} + \text{NaHCO}_3$ extractable PO_4^{3-} , $X_{\text{P}} =$
 749 20 – 90%, depending on soil texture), see SI S4 for calculations.

Sub-catchment	Fertiliser	$\delta^{18}\text{O}_{\text{P}(\text{export})}$ range	
		Fast+Slow ¹	→ Mostly slow ²
Pinjarra 19% clay, 4.4% loam, 76% sand	1 SP + 0 AG	17.7 – 21.3	18.5 – 20.5
	0.6 SP + 0.4 AG	18.7 – 21.9	19.1 – 22.6
Harvey 21% clay, 29% loam, 50% sand	1 SP + 0 AG	17.7 – 21.1	18.7 – 20.5
	0.6 SP + 0.4 AG	18.8 – 23.0	19.2 – 24.9

750 ¹ 50% ‘d’ + 50% ‘a’

751 ² 90% ‘d’ + 10% ‘a’

752

753

754

755

756

757

758

759

760

761

762

763

764

765

766

767

768 **Figure captions**

769 **Fig. 1** Two-pool isotope mixing models (Eq. 2, Eq. 3) constrained the possible $\delta^{18}\text{O}_\text{P}$ range of PO_4^{3-}
770 exported (leaching, run-off) from fertilised soils ($\delta^{18}\text{O}_{\text{P}(\text{export})}$). The model was solved using
771 recommended low, moderate, and high fertiliser applications rate (P_{fert} , in $\mu\text{g P g}^{-1}$ soil) for each soil
772 texture (clay, loam, sand) and $\delta^{18}\text{O}_{\text{P}(\text{fert})}$ values for two fertilisers (AG: N-P-K, SP: superphosphate)
773 manufactured between 2013 and 2017. $\delta^{18}\text{O}_{\text{P}(\text{fert})}$ for each year \times fertiliser were ‘mixed’ with each
774 soil texture using the measured $\delta^{18}\text{O}_{\text{P}(\text{soil})}$ range for P_{TIP} and P_{soil} ($\mu\text{g P g}^{-1}$ soil), defined by H_2O
775 extractable PO_4^{3-} for fast export scenarios (a, c) and $\text{H}_2\text{O} + \text{NaHCO}_3$ extractable PO_4^{3-} for
776 slow/seasonal export scenarios (b, d). $\delta^{18}\text{O}_{\text{P}(\text{export})}$ for both fast and slow export was calculated with
777 (c, d) and without (a, b) soil biological P turnover (X_P), which shifts $\delta^{18}\text{O}_{\text{P}(\text{export})}$ towards $\delta^{18}\text{O}_{\text{P}(\text{eq})}$
778 (Eq. 1). Fast export X_P (c) was approximated by $[P_{\text{H}_2\text{O}} \cdot e^{\wedge}(\log(100+P_{\text{H}_2\text{O}})/100 \cdot 1)]/P_{\text{TIP}}$ and slow
779 export X_P (d) by $[P_{\text{NaOH}} \cdot e^{\wedge}(\log(100+P_{\text{NaOH}})/100 \cdot 1)]/P_{\text{TIP}}$. Arrows indicate the same values were
780 applied across all soil textures, otherwise soil-specific values (mean \pm SD) were used. See SI S4 for
781 model scripts.

782

783 **Fig. 2** Phosphate in surface soils (0 – 10 cm) of 21 pastures with different textures in the Peel-
784 Harvey catchment (Western Australia) based on sequential extraction with H_2O (left, light outline),
785 NaHCO_3 , NaOH , and HCl (right, dark outline). P_{TIP} concentrations (sum of four fractions) for each
786 soil texture is indicated at the top, and the percentage contribution of H_2O (easily leachable) and
787 $\text{H}_2\text{O}+\text{NaHCO}_3$ (seasonally leachable) fractions indicated with dashed lines. Boxes represent median
788 ± 1 SD.

789

790 **Fig. 3** The $\delta^{18}\text{O}_\text{P}$ of P_{TIP} in pasture soils (0-10 cm) classed as either clay, loam, or sand from six
791 farms across the Peel-Harvey catchment (Western Australia). Boxes represent median ± 1 SD for
792 each soil texture. Black lines represent the mean (solid line), ± 1 SD (dashed lines), and

793 minimum/maximum (dotted lines) of the long-term local $\delta^{18}\text{O}_{\text{P(eq)}}$ range (Eq. 2); the grey line
794 indicates the mean $\delta^{18}\text{O}_{\text{P(eq)}}$ calculated for conditions during the winter sampling (*eq-w*).
795

796 **Fig. 4** The possible range of the isotopic composition of PO_4^{3-} export from clay, loam, and sand
797 pasture soils ($\delta^{18}\text{O}_{\text{P(export)}}$, ‰ v. VSMOW) within a catchment depends on fertiliser contribution to
798 the leachable soil PO_4^{3-} pool (f_{fert}) and fertiliser $\delta^{18}\text{O}_{\text{P}}$ composition (AG: black circles, SP: grey
799 triangles, manufactured 2013-2017). $\delta^{18}\text{O}_{\text{P(export)}}$ values were calculated for two export scenarios:
800 fast (a, c, e), where PO_4^{3-} is exported <1 day after fertilisation, and slow (b, d, f), where PO_4^{3-} is
801 leached over weeks-months. Both fast and slow export could occur with (e, f: $X_{\text{P}} = 1 \text{ h or 1 month}$)
802 or without (c, d: $X_{\text{P}} = \text{nil}$) soil biological P turnover (Eq. 3). Violins (a, b) show the distribution of
803 f_{fert} values around the mean (solid line); boxes (c-f) show the mean $\pm 1 \text{ SD}$ for $\delta^{18}\text{O}_{\text{P(export)}}$, with
804 whiskers to the minimum and maximum. Box colours distinguish soil textures (as defined in a and
805 b) and outlines the fertiliser (AG: black, SP: grey).

806